10B.4 POLARIMETRIC SIGNATURES OF MELTING HAIL AT S AND C BANDS: DETECTION AND SHORT-TERM FORECAST

JOSEPH C. PICCA* AND ALEXANDER V. RYZHKOV
Cooperative Institute for Mesoscale Meteorological Studies, University of Oklahoma, and NOAA/OAR National Severe Storms Laboratory, Norman, OK

1. INTRODUCTION

Dual-polarized radar has many advantages in diagnosing and predicting hazardous weather, in addition to its enhanced hydrometeor classification abilities. For example, the development and intensification of a thunderstorm can be recognized through various polarimetric variables, as they can identify different regions of the thunderstorm such as the updraft, downdraft, etc. With this identification, these regions can be monitored for development; subsequently, short-term forecasts for individual thunderstorms can be improved.

Previous work has effectively demonstrated hail detection using S-band polarimetric radar (e.g., Heinselman and Ryzhkov 2006). However, polarimetric variables also appear to show both a predictive and greater diagnostic capability for hail storms. Comparisons between S and C band data of hailstorms can provide further insight into what type of precipitation the observed polarimetric variables are representing. Scattering properties of hailstones (both wet and dry) differ between the two wavelengths. Observed differences can then assist in diagnosing the bulk properties of hydrometeors, such as melting hailstones, within a storm cell. Chiefly, the differences in cross-correlation coefficient (ρ_{hv}) and differential reflectivity (Z_{DR}) across the two bands are analyzed in following sections, which includes one unique event where both S and C band data from the same cell are directly compared.

The next focus is on the analysis of the hail core, extending from the growth region aloft through the precipitation core down to the surface. Past research has shown distinctive features of the growth region, where low values of ρ_{hv} indicate liquid water in a subfreezing region where wet hail growth is occurring (Ryzhkov et al. 2005; Kumjian and Ryzhkov 2008). The mixture of both liquid water and ice in this region allows water-coated hailstones to accumulate mass more rapidly than other regions of the storm cloud. Subsequently, as wet growth is the likely cause of most "giant" hailstones (4-5 cm and greater), there is much interest in the characteristics of this region. Furthermore, polarimetric variables can be analyzed in the hail core extending down from the growth region in order to determine the size and type of hailstones as they reach the surface. Balakrishnan and Zrnić (1990) first proposed the use of ρ_{hv} to aid in hail sizing, and our findings certainly show its utility in doing so. Through the investigation of ρ_{hv} and Z_{DR} in conjunction with the location of the hail core, a general idea of the hailstone characteristics can be ascertained, leading to improved diagnosis of hail size.

Finally, research has identified the "Z_{DR} column," a columnar region of high differential reflectivity in close proximity to a storm cell updraft, indicating a relatively high amount of liquid water from raindrops being lofted by the updraft (e.g., Caylor and Illingworth 1989; Meischner et al. 1991). Even though the raindrops themselves may not be the primary contributor to hailstone development, an increase in Z_{DR} likely indicates a strengthening updraft with a greater amount of cloud drops, which can significantly contribute to hail growth. Hence, the development of Z_{DR} columns in relation to storm strength and possible hail size is investigated.

Current hail detection consists of a WSR-88D algorithm that calculates the flux of hail kinetic energy and then applies a temperature-based weighting function to estimate a probability of hail and maximum size (Witt et al. 1998). As will be shown over the coming sections, polarimetric radar can improve upon this system through better diagnosis of hail sizes in different regions of a storm cell, as well as possibly providing a predictive capability through Z_{DR} columns.

1.1 S and C Band Hail Signatures Overview

Before examining the details of developing and melting hail, a brief overview of polarimetric hail signatures is provided at both wavelengths. Of note, however, S band is used for a "first look," as it is less affected by attenuation and resonant scattering. C-band signatures are then analyzed to transition into the comparison section.

The following S band data were collected by the research polarimetric prototype WSR-88D in

* *Corresponding author address*: Joseph C. Picca, 120 David L. Boren Blvd., National Weather Center Suite 4900, Norman, OK 73072. Email: jpicca@ou.edu

Norman, Oklahoma (KOUN). On 10 Feb 2009, several large supercell thunderstorms produced at least one tornado and hailstones upwards of 5 cm to the west and northwest of KOUN. One of the cells strongly exhibited several key polarimetric characteristics in large hail producing storms (Fig. 1). Widely observed in past research, we first note a clear hail signature of high reflectivity factor (Z_H) and low differential reflectivity (Z_{DR}) (Aydin et al. 1986) between 45 and 50 km in range (marked by "A") below the approximate environmental freezing level (indicated by the horizontal bar at 3 km height). This area is associated with the cell's hail core where severe hail certainly seems to exist. The second apparent signature is the Z_{DR} column ("B"), located around 45 km in range extending towards the freezing level, which indicates a large number of rain drops being lofted by a strong updraft. Finally, the area located above and to the right of the Z_{DR} column ("C") is distinguished by negative Z_{DR} and low ρ_{hv} (0.8-0.9), indicating a "mixed phase" region where both ice and liquid water are present and contributing to enhanced hail growth.

C-band data were collected by the King City, Ontario, Canada polarimetric radar. The day of 8 July 2007 saw a significant supercell develop to the west of the radar site, with hail reports upwards of 7 cm. Once again, we observe a region of high Z_H and low Z_{DR}, which indicates the hail core (Fig. 2). Furthermore, there is a very evident Z_{DR} column located around 115 km in range. However, we also note two key features in the data. First, the cross-section of Z_{DR} shows a drop in differential reflectivity behind the core (relative to the radar) at the lowest elevations, which is especially evident directly underneath the Z_{DR} column. This decrease is a result of differential attenuation in the precipitation core, which consists of melting hail and large rain drops that attenuate more of the horizontally polarized signal than the vertically polarized signal, resulting in decreased Z_{DR} values. Additionally, there is a region of very high Z_{DR} and low ρ_{hv} at the bottom of the precipitation core, which is a result of resonant scattering due to the effect of liquid drops from melting hail upon the shorter 5-cm wavelength of C band.

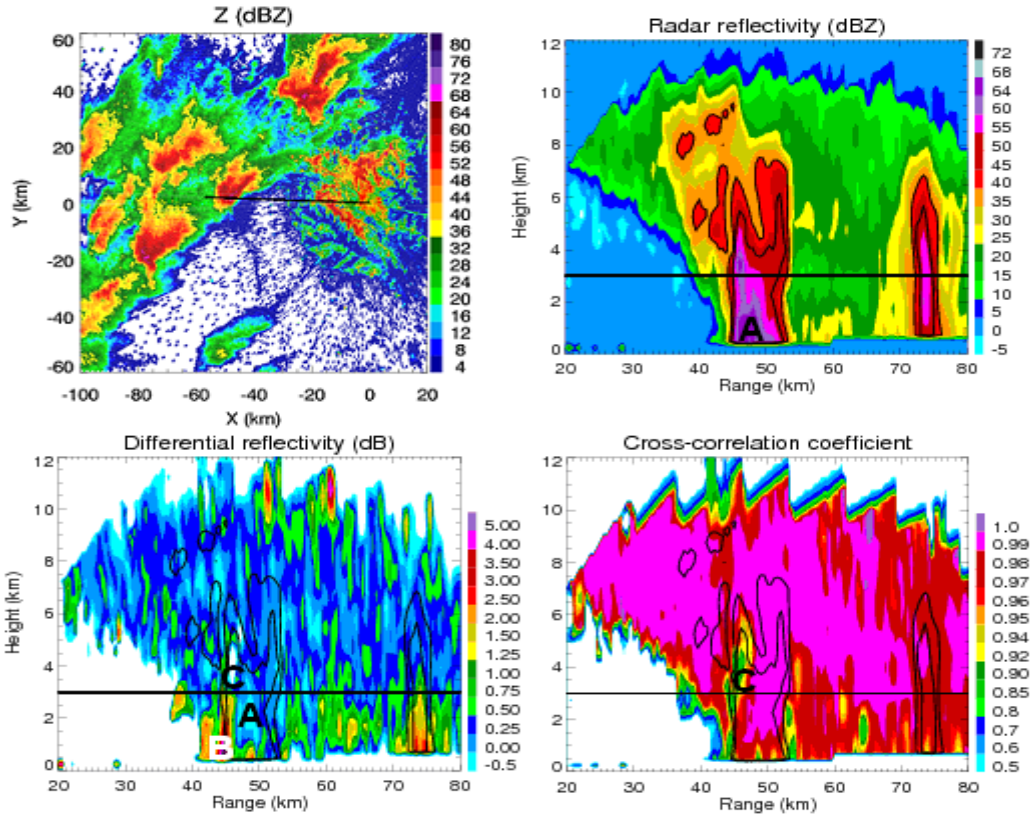

Fig. 1: KOUN (S band) 0.5˚ PPI of radar reflectivity factor Z_H (dBZ) from 10 Feb 2009 at 2114 UTC (upper left) and corresponding RHIs of radar reflectivity factor (upper right), differential reflectivity Z_{DR} (dBZ) (lower left), and cross-correlation coefficient ρ_{hv} (lower right). Cross-section contours indicate Z_H values of 40 and 50 dBZ.

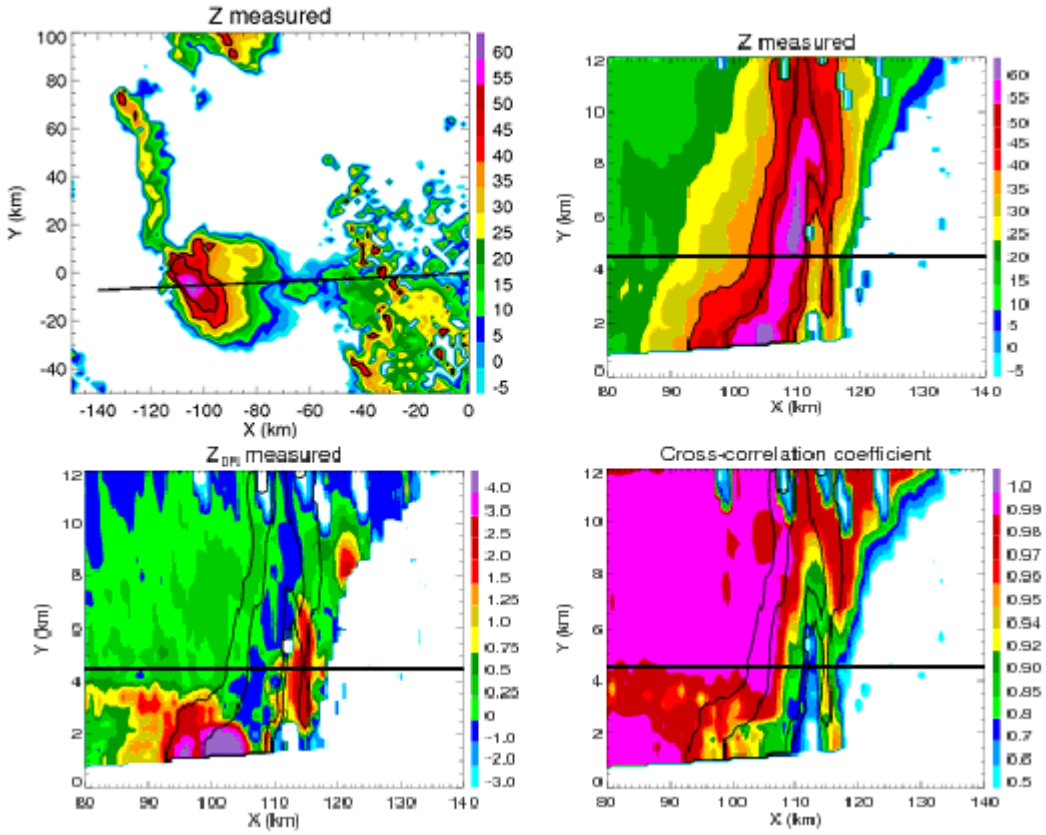

Fig. 2: King City, Canada (C band) 0.5˚ PPI of Z_H (upper left) from 8 July 2007 at 2310 UTC and corresponding RHIs (azimuth of 267˚) of Z_H (upper right), Z_{DR} (lower left), and ρ_{hv} (lower right). Cross-section contours indicate Z_H values of 40 and 50 dBZ.

In a modeling of Z_{DR} size dependencies for raindrops and melting hail, Borowska et al. (2010) display that the size of drops resulting from melting hail (around 6 mm in diameter) cause a spike in Z_{DR} at C band (Fig. 3) due to resonant scattering. In turn, this spike masks the lower Z_{DR} from the hailstones themselves, resulting in much higher Z_{DR} than is observed at S band. In the next section, we analyze a unique event where the two wavelengths can be directly compared, providing further support for these conclusions.

2. 27 MARCH 2009 S / C BAND COMPARISON

Norman, Oklahoma has the great fortune of being the home of both an S-band (KOUN) and a C-band (OU-PRIME) polarimetric radar. On 27 March 2009, a hailstorm (with 2-cm hail reported) developed to the southeast of Norman and was sampled by both radars. Although the volume scans were not synchronized, the high quality of data and relatively close temporal proximity of the scans allows for direct comparison.

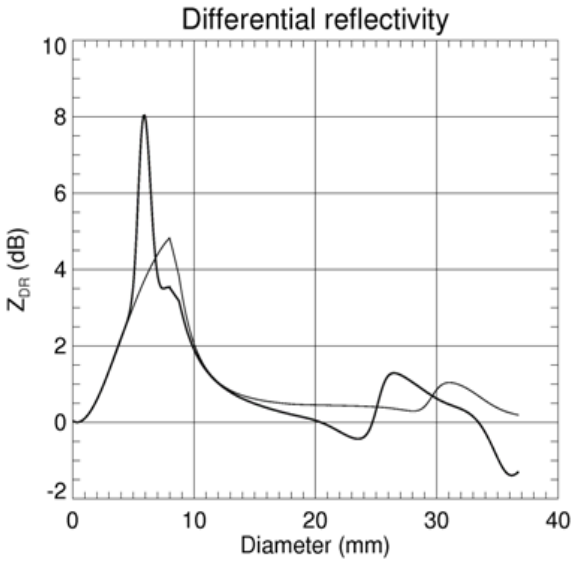

Fig. 3: Modeling of size dependencies of Z_{DR} at S (lighter line) and C (darker line) bands for raindrops and melting hail (Borowska et al. 2010).

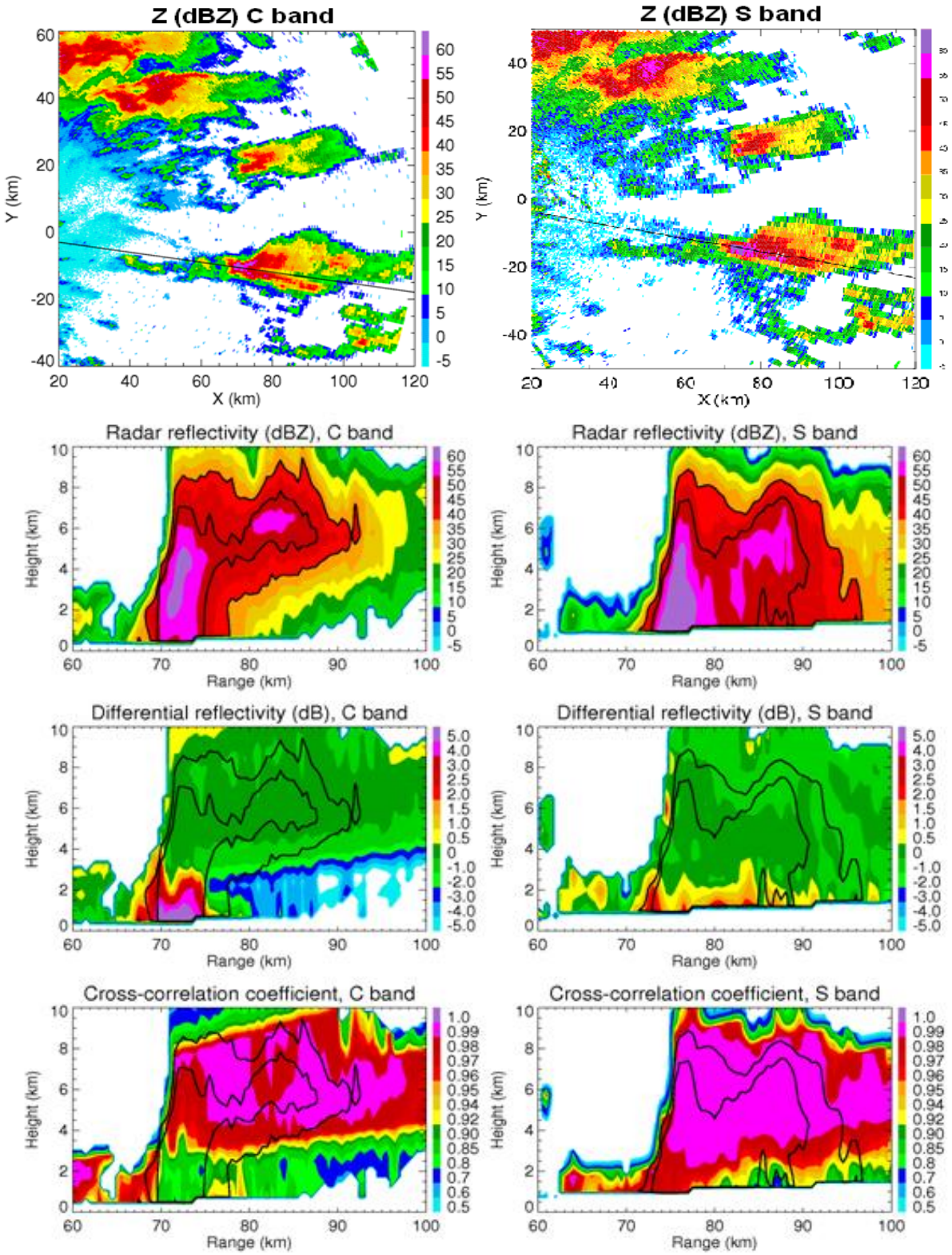

Fig. 4: OU-PRIME (C band) 0.5˚ PPI of Z_H (upper left) from 27 Mar 2009 at 1208 UTC and corresponding RHIs (azimuth of 98˚) of Z_H, Z_{DR}, and ρ_{hv} below the PPI, and KOUN (S band) 0.5˚ PPI of Z_H (upper right) at 1211 UTC and corresponding RHIs (azimuth of 101˚) of Z_H, Z_{DR}, and ρ_{hv} below the PPI.

Fig. 4 displays the lowest elevation scans of the two radars with the direction of subsequent RHI cross-sections indicated by the black lines, followed by the RHIs themselves that exhibit many of the features previously described. The first observation is the great attenuation of the radar signal due to heavy precipitation seen at C band. Whereas the S-band 40-dBZ Z_H contour extends over 20 km in width, it is not even 10 km in width at C band.

At S band, a hail signature is evident around 75 km range, where high Z_H coincides with a Z_{DR} depression that reaches the surface with an approximate value of 0.5 dB. For C band, this same region is located around 71 km range, but instead Z_{DR} values jump from near 0 dB around 2.5 km in height as one would expect with hail, to greater than 5 dB at the surface. The liquid drops due to melting hail in this region cause resonant scattering at the shorter wavelength of OU-PRIME, resulting in such a great jump in Z_{DR}. This conclusion is further supported by the very low ρ_{hv} also observed at C band, which is not seen in the S-band data.

The relatively high ρ_{hv} at S band throughout the core in addition to the previous observations supports a diagnosis that we are seeing small to marginally severe melting hail reaching the surface in this region of the cell. As a result, differential attenuation is once again evident at C band behind the core, where Z_{DR} values drop below 0 dB beneath an approximate altitude of 4 km.

Although maintaining both S and C band polarimetric radars in the same location is not feasible in an operational sense, the research field can shed light upon the bulk properties of hail cores by comparing different wavelengths. Subsequently, the information gained via research can be applied to the individual bands for deployment in operational algorithms.

3. VERTICAL PROFILES OF Z_{DR} AND ρ_{hv}

One of the great advantages of radar polarimetry is the ability to characterize hydrometeors in different areas of a cell. By analyzing the vertical profiles of polarimetric variables, hailstones can be tracked from their growth region all the way through their descent to the surface. The type of hail growth aloft can be determined and then applied to observations within the hail shaft to make an estimate of the size of hail reaching the surface.

On the evening of 29 May 2004, a powerful supercell thunderstorm tracked across central Oklahoma. Polarimetric data collected from the KOUN radar reveal very interesting and useful trends in the profiles. When combined with general knowledge for hail growth dependency on graupel / stone trajectories as well as some simple modeling, these trends have the potential to be utilized in an algorithm for improved hail sizing.

At 0117 UTC, both a PPI and RHIs of Z_H indicated the extreme likelihood that giant hail was present (Fig. 5). Furthermore, hail 7 cm in diameter was reported at 0110 UTC. Therefore, it is reasonable to assume that hail greater than 5 cm in diameter was falling within the reflectivity core. However, even within this region, changes in the polarimetric profiles are evident as the azimuth angle is shifted slightly to the right. The first RHI is at angle 314˚ and cuts through the region of the core where typically the largest hail falls. Research has shown these hailstones take an optimal trajectory within the supercell updraft, where liquid water and ice is available in a mixed phase region (Dennis and Musil 1973; Nelson 1983; Hubbert et al. 1998). Rapidly collecting both water and ice, they can grow to extreme sizes, assuming conditions are favorable, and then fall to the surface on the backside (west / northwest) of the updraft region. Analyzing the first RHI, we observe a clear hail signature of very low Z_{DR} (below -0.5 dB) within extremely high Z_H (over 70 dBZ) extending from the near-surface to well over the freezing level. Additionally, quite low ρ_{hv} (as low as 0.8) is noted throughout this signature.

These observations are consistent with observational and modeling studies of the wet growth region, especially when giant hailstones are present. Often near the top of the Z_{DR} column / updraft region, there exists a region of low Z_{DR} (sometimes negative) and low ρ_{hv}, occasionally less than 0.85 (Ryzhkov et al. 2005; Kumjian and Ryzhkov 2008). The low ρ_{hv} values appear to be associated with wet growth in the mixed phase region, as above the freezing level these values are a manifestation of liquid water in large drops or on hailstones. As wet hailstones approach resonant scattering sizes over 4-5 cm in diameter, not only is there a large decrease in ρ_{hv}, but also a significant decrease in Z_{DR}, as is evident by a simple modeling of Z_{DR} dependency on wet hail diameter (Fig. 6, courtesy of Matt Kumjian and Scott Ganson at NSSL).

Indeed, the observations from the 314˚ RHI show similar trends in ρ_{hv} and Z_{DR} within the extreme reflectivity region. Based upon the

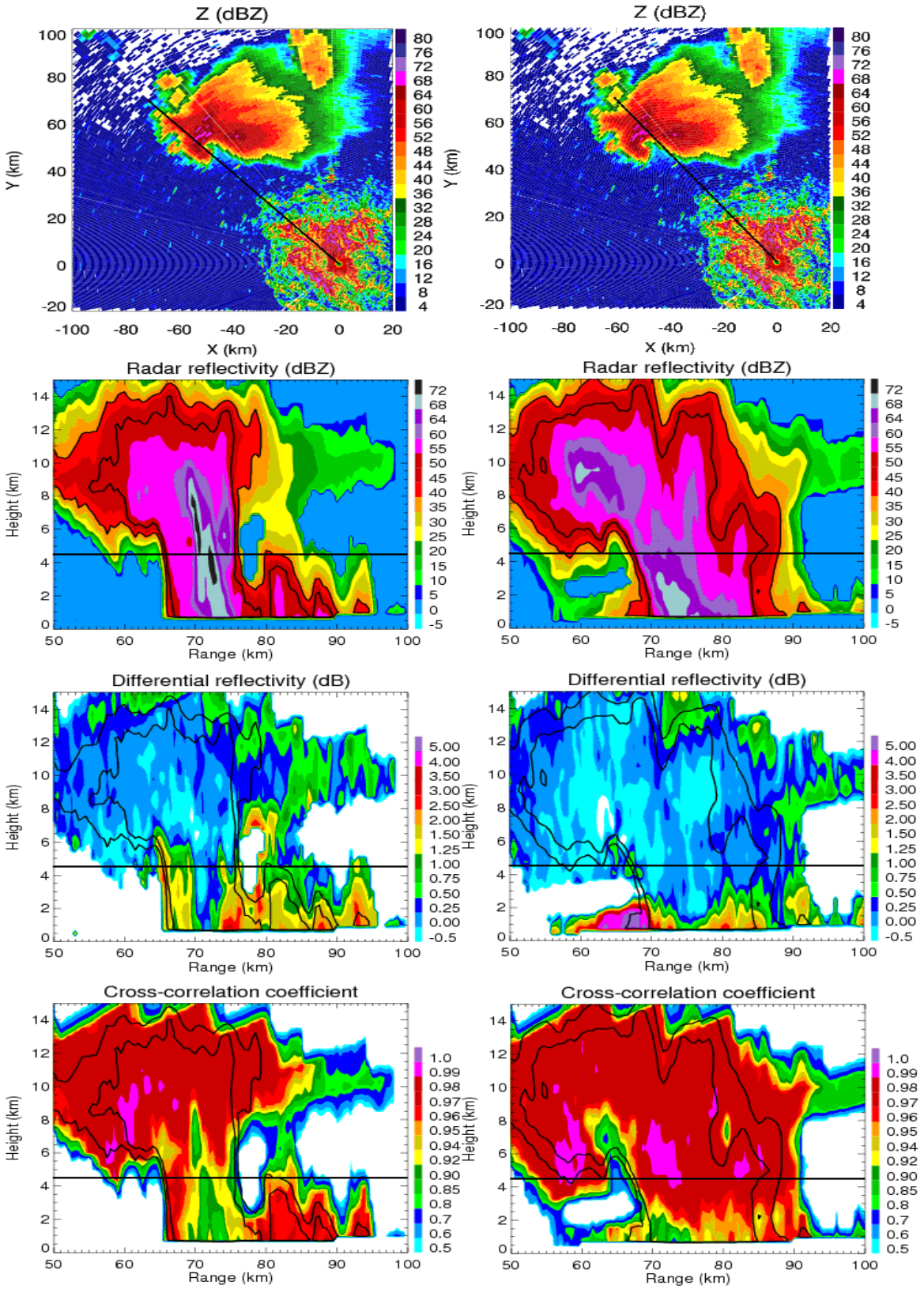

Fig. 5: KOUN 0.5˚ PPIs of Z_H from 30 May 2004 at 0117 UTC with indicated azimuths of 314˚ (upper left) and 317˚ (upper right) and their corresponding RHIs of Z_H, Z_{DR}, and ρ_{hv} below them for comparison.

vertical continuity of this region, as well as its position relative to the updraft, it seems very likely that the polarimetric data are indicating giant hailstones greater than 5 cm in diameter that experienced significant wet growth.

The importance of this analysis is magnified when viewing the 317˚ RHI at the same time. Although high Z_H is still observed, Z_{DR} values are slightly higher in the hail core than they were in the previous RHI. Even more noticeable is the great increase in ρ_{hv} within the core. Instead of values below 0.9 extending vertically from the surface through the freezing level, ρ_{hv} is very high (0.98-0.99) around the freezing level and only begins to decrease 2-3 km below this level. This signature is indicative of dry hail aloft that gains and then sheds liquid water as it melts below the freezing level. Furthermore, the location of the highest reflectivity in this RHI is farther from the mixed phase region of the updraft where one would expect the largest hailstones to grow. Therefore, the much higher ρ_{hv} and slightly higher Z_{DR} appears to be indicating dry hailstones that are still significant (possibly 4-5 cm in diameter), but not of the size most likely observed with the previous RHI.

It cannot be emphasized enough that hail growth and fall trajectories happen in a three-dimensional nature. Therefore, any one RHI "slice" does not depict the full trajectory of a region of hailstones. Nonetheless, by analyzing both observational and model polarimetric data in relation to accepted knowledge for hailstone trajectories, these RHIs do display several useful trends for hail sizing. The largest hail (over 5 cm) appears to be associated with negative Z_{DR} and low ρ_{hv} (below 0.9), especially if wet. If the hail is dry, even larger sizes (6-7 cm and greater) are necessary to reduce ρ_{hv} via resonant scattering. Generally though, high ρ_{hv} is associated with dry hail around 5 cm in diameter and smaller. With these hailstones, as Z_{DR} increases from near 0 dB to higher values, the associated hail diameter decreases.

With further modeling and observational analysis, these trends can likely be applied in a hail-sizing algorithm more accurate and region-specific than the current WSR-88D algorithm.

4. Z_{DR} COLUMNS AS A PREDICTIVE TOOL

Within a storm updraft, raindrops are lofted to altitudes sometimes extending several kilometers above the freezing level. If the strength of the updraft is such that large raindrops can be lofted, their oblate spheroid shape causes a columnar

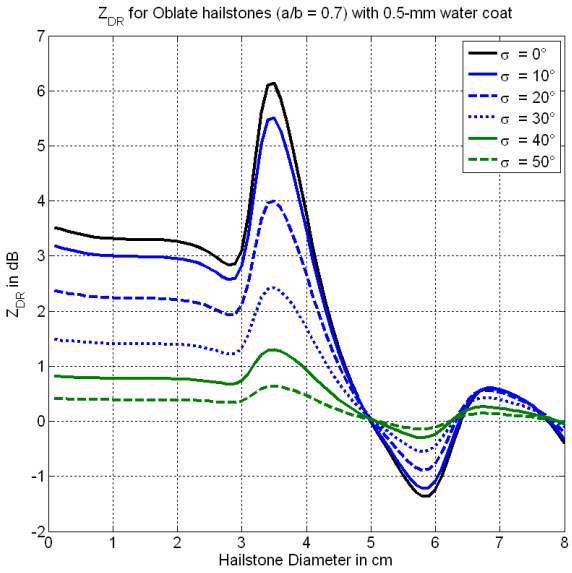

Fig. 6: Modeling of size dependencies of Z_{DR} for wet hailstones. The width of the canting angle distribution is indicated in the upper right corner.

region of increased Z_{DR} values anywhere from 1 dB to occasionally over 5 dB (at S band).

Intuitively, a stronger updraft can loft larger raindrops with higher intrinsic Z_{DR} values to greater altitudes. Therefore, one may expect with increasing Z_{DR} in a growing column that the storm updraft is intensifying and, subsequently, heavier precipitation and possibly larger hail could be expected to develop in the near future. Although large raindrops do not appear to be the primary contributor to large hail growth, they can reveal a strengthening updraft that has a growing number of cloud drops which can contribute significantly to hail growth (Askelson 2002). Hence, Z_{DR} columns offer a possibility for improved short-term prediction of hail trends within storm cells.

For our purposes, we analyze a supercell that tracked across northern Oklahoma during the afternoon and evening of 24 May 2008, producing several tornadoes. Although there were no official hail reports, KOUN Z_H plots (Fig. 7) show that at least marginally severe hail (at least 2 cm) was likely.

The cross-section at 2242 UTC displays a couple of important features that have been previously discussed as possible indicators of increasing hail growth. First, a clear Z_{DR} column is located at 108 km range and extends over 2 km above the environmental freezing level. Additionally, near the top of this column, we observe an area of decreased ρ_{hv} (as low as 0.92). These signatures signal the presence of a strong updraft that is promoting wet hail growth in a

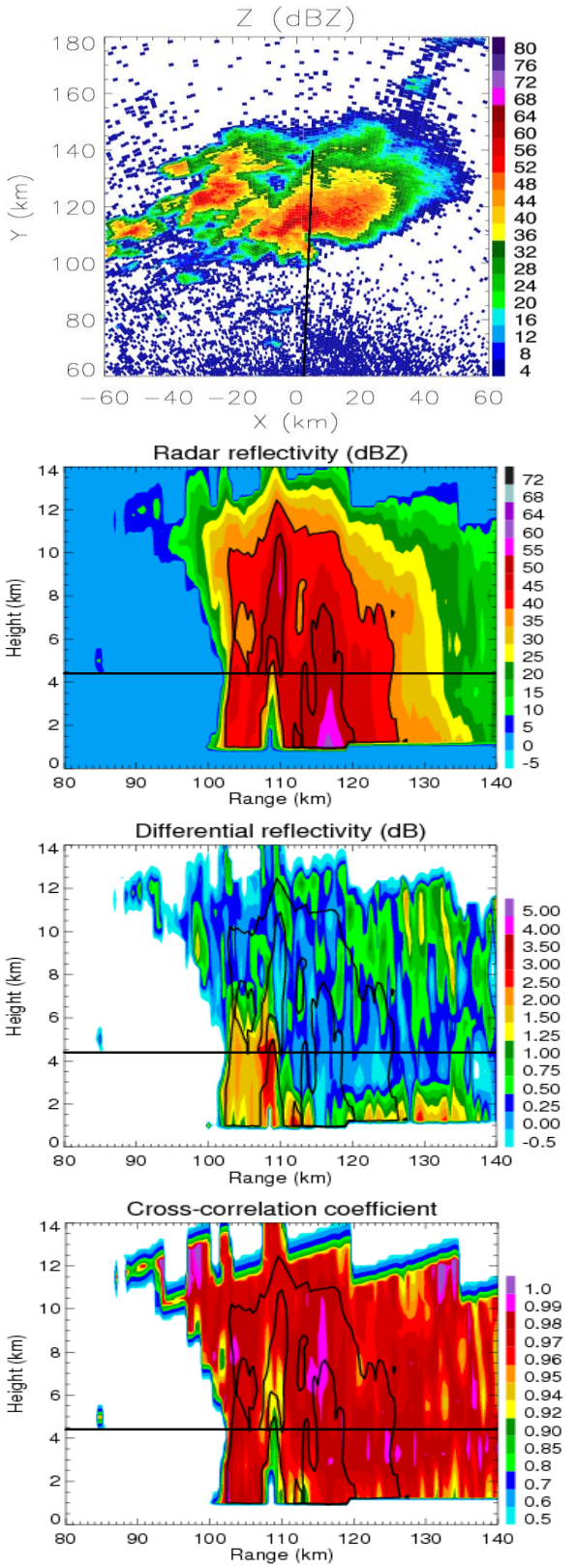

Fig. 7: KOUN 0.5˚ PPI of Z_H from 24 May 2008 at 2242 UTC and corresponding RHIs (azimuth of 2˚) of Z_H, Z_{DR}, and ρ_{hv} below the PPI.

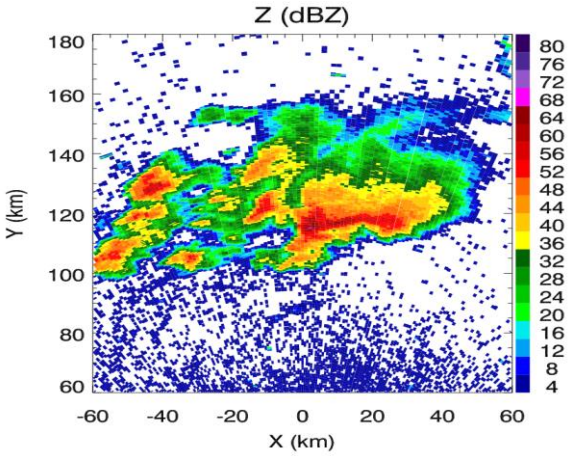

Fig. 8: KOUN 0.5˚ PPI of Z_H from 24 May 2008 at 2309 UTC.

mixed phase region. Therefore, we may reasonably expect to see high reflectivity at the lowest elevation angle within the next 15 to 30 minutes, which generally agrees with past findings for hail growth and fall time (e.g., Foote 1983). Qualitatively, Fig. 8 supports our expectation as Z_H values within the core have increased to over 65 dBZ at the lowest elevation angle, indicative of large hail.

Although this qualitative analysis is helpful in supporting the predictive nature of Z_{DR} columns, further proof is required to show their utility. Therefore, quantitative measures of the intensity of both the Z_{DR} column and the reflectivity core were developed. To do so, from 2221 to 2345 UTC each KOUN volume scan (approximately every 6 minutes) was fit to a Cartesian grid. Constant Altitude PPIs were then produced for every 250 meters in height. Above the environmental freezing level, each grid box that met a certain Z_{DR} threshold (at least 1, 2, or 3 dB) was counted in a Z_{DR} column volume. Below this level, the same was done for grid boxes that met or exceeded thresholds of 40 or 60 dBZ. The ratio of the 60 dBZ volume to the 40 dBZ volume was then used as a proxy for reflectivity core intensity. The results were then plotted as a time series (Fig. 9), which reveals a noticeable trend: for each "boost" in Z_{DR} column volume (especially when considering the 1 dB threshold), we observe an increase in the Z_H ratio approximately 15 to 25 minutes later, which falls in line with expected hail growth times.

Both the qualitative and especially the quantitative analyses indicate a lag correlation between Z_{DR} column strength and reflectivity core strength. Although these analyses need to be

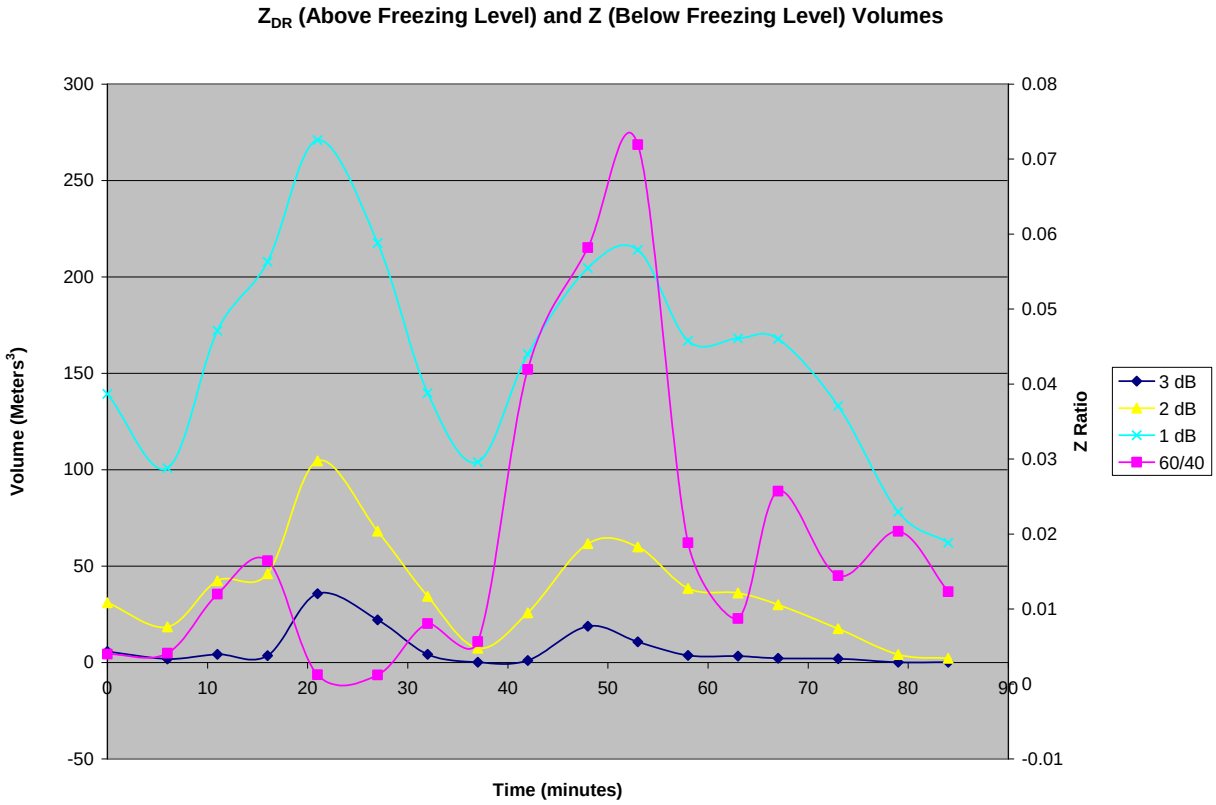

Fig. 9: Time series of Z_{DR} volumes and Z_H volume ratios from 24 May 2008 supercell between 2221 UTC and 2345 UTC, a span of 84 minutes.

performed on more cases, at least here it appears that Z_{DR} columns can provide an "early warning" for increasing hail growth. Forecasters could then use this signal to provide improved warnings for hailstorms. In turn, financial loss in various industries affected by hail could be greatly reduced. Certainly, this feature requires further consideration as it is associated with an integral part of storm structure—namely, the updraft—and, subsequently, the intensity of the storm.

4. SUMMARY AND CONCLUSIONS

Already well known, polarimetric radar offers great insight into hydrometeor classification within thunderstorms and in general. However, what is now becoming more apparent is its ability to diagnose the actual processes occurring within storm cells and their effect on hail growth. From the lofting and production of drops capable of enhancing growth to the growth itself and subsequent hail cascade to the surface, this data can be used to monitor hail size and perhaps forecast short-term changes in hail intensity. Additionally, unique opportunities exist in the comparison of S- and C-band data. The different scattering properties caused by the two wavelengths can improve our understanding of melting hail observation, which can then be applied to the individual wavelengths for operational purposes.

Within the United States, S-band signatures are of greatest importance, as the national WSR-88D network will be undergoing a polarimetric upgrade over the coming years. A great amount of promise lies in the diagnosis of hail characteristics via vertical profiles of ρ_{hv} and Z_{DR} within the hail cascade. Very large hail from the wet growth region near the updraft can be distinguished by low ρ_{hv} and Z_{DR} values extending from the ground to well over the freezing level. At the same time, high ρ_{hv} and slightly higher Z_{DR} values that decrease and increase, respectively, below the freezing level may indicate smaller dry hail that is gaining liquid water as it melts. In turn, these observations can allow forecasters and radar algorithms to identify accurately the general characteristics of different hail regions in a storm cell.

Lastly, Z_{DR} columns likely can be utilized to improve short-term prediction (15-30 minutes) of storm trends, including the possibility of more vigorous or weakening hail production. Trends in Z_{DR} values can serve as a proxy for updraft strength, and likely the availability of cloud drops for hail growth. Therefore, for example, with a signal of a strengthening Z_{DR} column, a forecaster could reasonably predict a short-term increase in reflectivity core intensity. Nonetheless, many more storms need to be analyzed in a similar fashion as was done here.

5. ACKNOWLEDGEMENTS

We would like to thank the NSSL/CIMMS and Atmospheric Radar Research Center employees whose work ensured data collection by KOUN and OU-PRIME at research-grade quality. Additionally, we thank David Hudak and Jim Young from Environment Canada for providing C-band polarimetric data collected by the King City radar. Funding for this study comes from NOAA/Univ. of Oklahoma Cooperative Agreement NA17RJ1227 under the U.S. Dept. of Commerce. We also acknowledge Matthew Kumjian and Scott Ganson at NSSL for their modeling work that enhanced this study.

6. REFERENCES

Askelson, M.A., 2002: Hydrometeor Structures Observed in Supercells. Ph.D. dissertation, University of Oklahoma, 246 pp.

Aydin, K., T. Seliga, and V. Balaji, 1986: Remote Sensing of Hail with a Dual Linear Polarization Radar. *J. Appl. Meteor.*, **25**, 1475-1484.

Balakrishnan, N., and D.S. Zrnić, 1990: Use of Polarization to Characterize Precipitation and Discriminate Large Hail. *J. Atmos. Sci.*, **47**, 1525-1540.

Borowska, L., A. Ryzhkov, D. Zrnić, C. Simmer, R. Palmer, 2010: Attenuation and Differential Attenuation of the 5-cm Wavelength Radiation in Melting Hail. *J. Appl. Meteor. Climatol.*, **submitted**.

Dennis, A., and D. Musil, 1973: Calculations of Hailstone Growth and Trajectories in a Simple Cloud Model. *J. Atmos. Sci.*, **30**, 278-288.

Foote, G.B., and H.W. Frank, 1983: Case Study of a Hailstorm in Colorado. Part III: Airflow from Triple-Doppler Measurements. *J. Atmos. Sci.*, **40**, 686-707.

Heinselman, P.L., and A.V. Ryzhkov, 2006: Validation of Polarimetric Hail Detection. *Wea. Forecasting*, **21**, 839-850.

Hubbert, J., V.N. Bringi, L.D. Carey, and S. Bolen, 1998: CSU-CHILL Polarimetric Radar Measurements from a Severe Hail Storm in Eastern Colorado. *J. Appl. Meteor.* **37**, 749-775.

Illingworth, A., and I. Caylor, 1989: Polarization Radar Estimates of Raindrop Size Spectra and Rainfall Rates. *J. Atmos. Oceanic Technol.*, **6**, 939-949.

Kumjian, M.R., and A.V. Ryzhkov, 2008: Polarimetric Signatures in Supercell Thunderstorms. *J. Appl. Meteor. Climatol.*, **47**, 1940-1961.

Meischner, P., V. Bringi, D. Heimann, and H. Höller, 1991: A Squall Line in Southern Germany: Kinematics and Precipitation Formation as Deduced by Advanced Polarimetric and Doppler Radar Measurements. *Mon. Wea. Rev.*, **119**, 678-701.

Nelson, S.P., 1983: The Influence of Storm Flow Structure on Hail Growth. *J. Atmos. Sci.*, **40**, 1965-1983.

Ryzhkov, A.V., T.J. Schuur, D.W. Burgess, P.L. Heinselman, S.E. Giangrande, and D.S. Zrnić, 2005: The Joint Polarization Experiment: Polarimetric Rainfall Measurements and Hydrometeor Classification. *Bull. Amer. Meteor. Soc.*, **86**, 809-824.

Witt, A., M.D. Eilts, G.J. Stumpf, J.T. Johnson, E.D. Mitchell, and K.W. Thomas, 1998: An Enhanced Hail Detection Algorithm for the WSR-88D. *Wea. Forecasting*, **13**, 286-303.